Journal of Fluids and Structures (1997) **11,** 345–350

SPECIAL BRIEF NOTE

MEASURING INSTANTANEOUS FLUID DYNAMIC FORCES ON BODIES, USING ONLY VELOCITY FIELDS AND THEIR DERIVATIVES

F. Noca, D. Shiels and D. Jeon
Graduate Aeronautical Laboratories, California Institute of Technology, m/s 205–45 Pasadena, CA 91125, U.S.A.

(Received 7 November 1996 and in revised form 20 January 1997)

We present an exact expression for the evaluation of instantaneous forces on a body in an incompressible cross-flow which only requires the knowledge of the velocity and vorticity field in a finite and arbitrarily chosen region enclosing the body. This expression is particularly useful for experimental techniques like Digital Particle Image Velocimetry (DPIV) which provide instantaneous, 2-D velocity and vorticity fields but not pressure fields. The present formula is tested on a numerical flow simulation using a high-resolution vortex method and experimentally with DPIV on a circular cylinder flow.

1. INTRODUCTION

Relating the unsteady loading on a bluff-body structure with the associated wake is an ongoing research effort in the fluid mechanics community. With the advent of Digital Particle Image Velocimetry (DPIV), wake studies have been taken up to a new level, thanks to spatiotemporal investigations which are now part of laboratory routine. The question still remains whether the measurement of spatial distributions of vorticity at different instants of time can lead to an evaluation of the forces acting on a body.

In Computational Fluid Dynamics (CFD), two common methods for calculating forces are the direct evaluation of the pressure and the shear stress on the surface of the body and the concept of the fluid dynamic impulse over the entire vorticity field. The former method is difficult to apply because of the need to resolve the boundary layers on the body fully, where the velocity and vorticity gradients are very large. The latter method has been applied in an experiment by Lin & Rockwell (1996) on the loading of an oscillating cylinder in quiescent water. Starting the cylinder from rest, they studied the flowfield at early times to help confine the vorticity to a small domain surrounding the body. However, in most experimental cases, it is rare for vorticity to be confined to a finite domain.

To remove some of the constraints imposed by these two methods, we present an exact formulation for the calculation of unsteady forces in incompressible, viscous, and

0889–9746/97/030345 + 06 $25.00/fl970081

rotational flows, which relies only on the flowfield in a finite, arbitrarily chosen domain surrounding the body.

2. FORMULATION

As it often occurs in science, some results are often forgotten and are subject to rediscovery. The formulation we are presenting is one such case.

The complete formulation for viscous and rotational flows was already given by Moreau (1952), but the author quickly turned his attention to a particular form of his equation, which was related to the fluid dynamic impulse concept and which could be handled analytically for simple and inviscid flow cases. Saffman (1993) presented an inviscid form of this formulation, but the reader may be left with the wrong impression that this formulation has no relevance for viscous flows. It turns out that the Saffman approach can be very accurate because the viscous terms are often negligible.

A complete and clearer derivation of the general formulation is given by Noca (1996), and the result is described herein. The starting point for the force $\mathbf{F}$ is a control-volume approach for momentum conservation:

$$\mathbf{F} = -\frac{\mathrm{d}}{\mathrm{d}t}\int_{V_m(t)} \rho\mathbf{u}\,\mathrm{d}V + \oint_{S_m(t)} \mathbf{n}\cdot\boldsymbol{\Sigma}\,\mathrm{d}S, \tag{1}$$

where ρ is the fluid density and is taken equal to unity, $\mathbf{u}$ its velocity, and $\boldsymbol{\Sigma}$ the stress tensor. Here, the material volume $V_m(t)$ is bounded by an inner surface (corresponding to the body surface) and an outer material surface $S_m(t)$, with outward unit normal $\mathbf{n}$, chosen at will. Note that the stress tensor includes the pressure term. After some lengthy algebraic manipulations (Noca 1996), the pressure term can be eliminated, and the resulting force equation can be broken down into the sum of a volume integral and a surface integral, plus an extra term which describes the unsteady motion of the body surface $S_b(t)$:

$$\mathbf{F} = -\frac{1}{N-1}\frac{\mathrm{d}}{\mathrm{d}t}\int_{V(t)} \mathbf{x}\times\boldsymbol{\omega}\,\mathrm{d}V + \oint_{S(t)} \mathbf{n}\cdot\boldsymbol{\Theta}\,\mathrm{d}S - \frac{1}{N-1}\frac{\mathrm{d}}{\mathrm{d}t}\oint_{S_b(t)} \mathbf{x}\times(\mathbf{n}\times\mathbf{u})\,\mathrm{d}S, \tag{2}$$

where N is the dimension of the space under consideration ($N = 2$ in a two-dimensional space) and $\boldsymbol{\omega}$ the vorticity. The tensor $\boldsymbol{\Theta}$ is given by

$$\begin{aligned}\boldsymbol{\Theta} = {} & \frac{1}{2}u^2\mathbf{I} - \mathbf{u}\mathbf{u} - \frac{1}{N-1}(\mathbf{u}-\mathbf{u}_s)(\mathbf{x}\times\boldsymbol{\omega}) + \frac{1}{N-1}\boldsymbol{\omega}(\mathbf{x}\times\mathbf{u}) \\ & + \frac{1}{N-1}[\mathbf{x}\cdot(\boldsymbol{\nabla}\cdot\mathbf{T})\mathbf{I} - \mathbf{x}(\boldsymbol{\nabla}\cdot\mathbf{T})] + \mathbf{T},\end{aligned} \tag{3}$$

where $\mathbf{T}$ is the *viscous* stress tensor. Note that we chose to write this expression using an arbitrary (non-material) volume $V(t)$ bounded by a (non-material) surface $S(t)$ moving with velocity $\mathbf{u}_s$. If the surface $S(t)$ is taken to infinity such that it encloses the whole vorticity field—and, in two dimensions, if there is no net circulation around the body—then the surface integral vanishes and we recover the force as the time derivative of the hydrodynamic impulse (for a body in steady motion).

Relation (2) can be put in yet another form, similar to Saffman (1993), by converting some of the surface integral terms to a volume integral. For the case of a nonrotating, solid cylinder, that transformation is as follows:

$$\oint_{S(t)} [\tfrac{1}{2}u^2\mathbf{n} - (\mathbf{n}\cdot\mathbf{u})\mathbf{u}]\,\mathrm{d}S = \int_{V(t)} \mathbf{u}\times\boldsymbol{\omega}\,\mathrm{d}V. \tag{4}$$

Both versions of the equations were used in our experiments.

3. NUMERICAL AND PHYSICAL EXPERIMENTS

High-resolution CFD provided a good means for testing the proposed force relation given by equation (2). In this work, a particle-based vortex method (Koumoutsakos & Leonard 1995) is used for simulation of flow over an oscillating cylinder. In this discussion we shall consider three methods for computing forces: (A) the fluid dynamic impulse (i.e. the integral of the first moment of the vorticity field); (B) direct pressure and shear stress calculation; and (C) the new formulation based on equation (2). Requiring neither the knowledge of the entire vorticity field (A), nor the numerically difficult evaluation of the large vorticity gradients near the body (B), method C can be preferable to A & B with no loss of accuracy.

The test case was for an incompressible, 2-D flow over a circular cylinder with $\mathrm{Re} = 392$. The cylinder was oscillated normal to the flow direction with velocity $\sin(4\pi t/13)$ to induce a strongly varying flowfield (our lengths were scaled by the cylinder diameter and velocities by the freestream velocity). The cylinder traveled 12 diameters downstream from an impulsive start, resulting in the vorticity field in Figure 1(a). A time step of $\mathrm{d}t = 0{\cdot}0075$ was used, and spatial resolution of approximately (in a Lagrangian sense) $\mathrm{d}x \simeq 0{\cdot}004$ was maintained.

Methods A and B have been verified in Koumoutsakos & Leonard (1995) for this class of flows. The natural means of discretizing Method C for the computation used the particle locations (and assumed Gaussian basis functions) for volume integrals along with a bounding box to represent the surface $S(t)$, as shown in Figure 1(a). The bounding box is considered to move with the flow ($\mathbf{u}_s = \mathbf{u}$) for computation of the time derivative and has a spacing of $\mathrm{d}h = \mathrm{d}x$ (fine resolution) or $\mathrm{d}h = 10\,\mathrm{d}x$ (coarse resolution). The results of the fine resolution are shown in Figure 1(b), showing good agreement with methods A & B. The computation of lift using a fine resolution grid to discretize equation (2), rather than the particle locations, results in the points plotted in Figure 1(b). Good agreement is again evident. It was found, however, that results using a coarse resolution grid exhibited a good deal of error, unlike the plotted cases. The results were insensitive to the size and velocity of the bounding boxes. These observations on the effectiveness of Method C for extracting lift also held for determining the drag coefficient.

For the physical experiment, we chose to validate this technique on a cylinder wake flow. The cylinder was attached to a two-component force balance and placed in a water tunnel at $\mathrm{Re} = 19\,000$ to ensure a strong lift signal for the balance. The flow field was measured with a DPIV system, allowing us to make instantaneous 2-D flow field measurements at midspan. Our measurement box spanned from $-1 < x < 1{\cdot}75$ in the streamwise direction and $-1 < y < 1$ in the cross-stream direction, and did not include the large-scale vortex structures, which form further downstream. The force formula requires flow data all around the cylinder, thereby necessitating the use of glass cylinders for seamless illumination. We synchronized both data systems and collected data over 31 diameters of downstream motion, about 7·5 shedding cycles. Direct

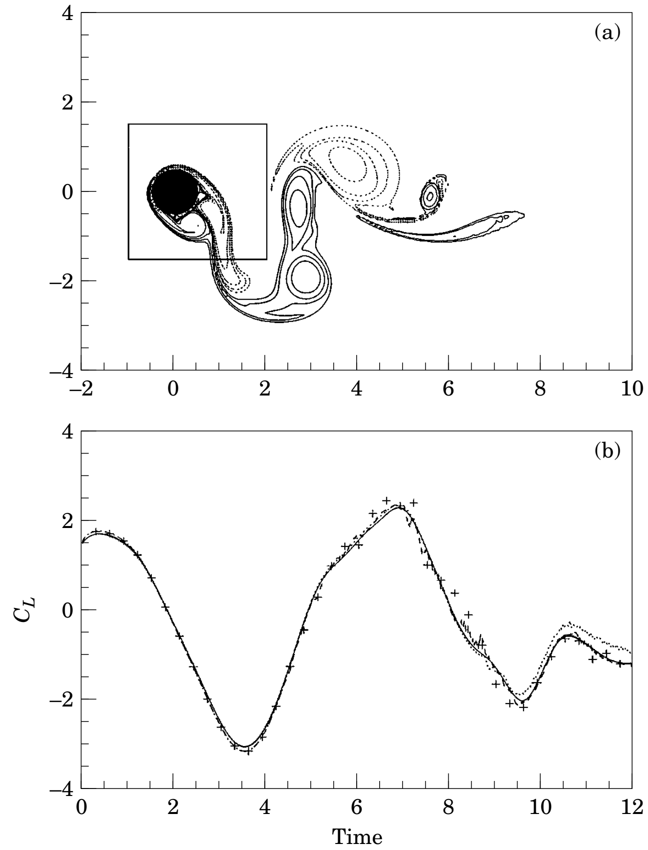

Figure 1. (a) Vorticity field from computations with bounding box for force calculations. (b) Comparison of lift forces obtained by several methods: · · ·, Method A (*fluid-dynamic impulse method*); —, Method B (*pressure and shear stress on body*); - - -, Method C (*present formulation*); + + +, gridded Method C (*present formulation on regularly gridded data*).

application of equation (2) yielded noisy results. While the viscous stress terms were essentially negligible, the time derivative of the hydrodynamic impulse term was very noisy in front of the cylinder. We attribute this problem to under-resolving the forebody boundary layer. Unlike the CFD study, we could only resolve to $dt \simeq 0{\cdot}1$ and $dx \simeq 0{\cdot}03$. Since the vorticity in the boundary layer is much larger than in the wake, any error here is greatly amplified. However, since this part of the flowfield is nearly steady, an assumption which is clearly not valid for moving bodies, we removed the time-derivative contributions from this region.

After applying these corrections, the final result is presented in Figure 2, along with the lift signal measured with the force balance. We note several important features:

1. Whereas the force balance measures a *spanwise-averaged* force, the formulation essentially yields a *sectional* force since it is evaluated with data taken only at midspan. However, since we are using a 2-D formulation on a 3-D flowfield, we expect this is not the exact sectional force.

2. The lift signal from the formulation and the force balance have the same *period.*

3. The *amplitude* of the sectional lift tends to be higher and the signal more irregular

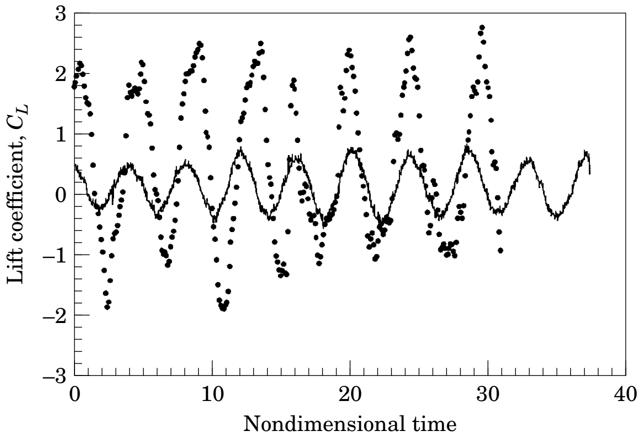

Figure 2. Comparison of experimental lift forces: · · · , present formulation using DPIV data (*sectional lift*); —, force balance (*spanwise-averaged lift*).

than the lift from a force balance. This is thought to arise from spanwise phase variations in the vortex shedding, as documented by Szepessy & Bearman (1992). The spanwise averaging by the force balance yields a lower amplitude signal because local spanwise variations will tend to cancel each other.

4. These spanwise variations (Szepessy & Bearman 1992) also are related to the *phase* variations of the sectional lift. Figure 2 shows that from time 0–15, sectional lift leads the force-balance lift, whereas from time 15–27 they are in phase. At time 27 the sectional lift again jumps ahead in phase. Meanwhile the force-balance signal has been constant in phase.

5. Both signals show a positive mean value. Because we used a large diameter cylinder (11 cm diameter model in a 50×50 cm water tunnel), we believe that a slightly off center location of the cylinder resulted in this asymmetry. Nevertheless these two signals are consistent with each other in this regard.

4. CONCLUSION

We have presented an exact expression for evaluating body forces from only velocity and vorticity data. With the availability of computational fluid dynamics and instantaneous velocity field measurements, this expression can now be fully exploited for force measurements. The primary advantage of this formulation is the minimal list of assumptions required for accurate measurement. Requiring neither pressure fields and shear stresses on the body nor knowledge of the entire flow field, this formula seems to be particularly useful and simple to implement. As we have shown, the formula is quite accurate for fully resolved computational results, and surprisingly informative even for the under-resolved experimental data presented here. As technological advances improve spatial and temporal resolution, this formula will surely become increasingly useful for experimental force measurement. Even for computational studies, this formulation has proved to be a useful alternative. Because the velocity and vorticity fields are readily measurable, both experimentally and numerically, the formula is immediately useful for force measurements.

ACKNOWLEDGEMENTS

We wish to acknowledge the generous support of the Office of Naval Research under grants, N00014-93-1144 & N00014-94-1-0793, the Jet Propulsion Laboratory Supercomputing Project (funded from the NASA Offices of Mission to Planet Earth) for computer time, and the gracious guidance of our respective advisors, Professors A. Roshko, A. Leonard and M. Gharib.

References

Koumoutsakos P. & Leonard, A. 1995 High-resolution simulations of the flow around an impulsively started cylinder using vortex methods. *Journal of Fluid Mechanics* **296,** 1–38.

Lin, J. C. & Rockwell D. 1996 Force identification by vorticity fields: techniques based on flow imaging. *Journal of Fluids and Structures* **10,** 663–668.

Moreau J. J. 1952 Bilan dynamique d'un écoulement rotationnel. *Journal de Mathématiques Pures et Appliquées* **31,** 355–375; **32,** 1–78.

Noca F. 1996 *On the evaluation of instantaneous fluid-dynamic forces on a bluff body.* GALCIT Report FM96-5.

Saffman P. E. 1993 *Vortex Dynamics.* Cambridge: Cambridge University Press.

Szepessy S. & Bearman P. W. 1992 Aspect ratio and end plate effects on vortex shedding from a circular cylinder. *Journal of Fluid Mechanics* **234,** 191–217.

Willert C. & Gharib M. 1991 Digital particle image velocimetry. *Experiments in Fluids* **10,** 181–193.